The Journal of Experimental Biology 205, 2943–2954 (2002)
Printed in Great Britain © The Company of Biologists Limited 2002
JEB4313

Mechanisms of acid secretion in pseudobranch cells of rainbow trout *Oncorhynchus mykiss*

G. Kern, S. T. Bösch, E. Unterhuber and B. Pelster*

Institut für Zoologie und Limnologie, Universität Innsbruck, Technikerstrasse 25, A-6020 Innsbruck, Austria

*Author for correspondence (e-mail: Bernd.Pelster@uibk.ac.at)

Accepted 14 June 2002

Summary

Cell suspensions of rainbow trout *Oncorhynchus mykiss* pseudobranch, prepared by Ca^{2+} depletion and mechanical maceration, contained a distinct population of cells that always kept their relatively cuboidal shape and did not round up in suspension or proliferate after adhering to the surface of cell culture dishes. Phase-contrast microscopy revealed an extensive system of basal membrane invaginations, and Na^+-K^+-ATPase- and anion-exchanger-like immunoreactivity could be localized in cell membranes. The cells were characterized by a high mitochondrial density. Using specific antibodies, V-ATPase subunit B was localized in the plasma membrane. Using a cytosensor microphysiometer, the rate of acid secretion of these cells was measured and compared with the activity of a gill cell preparation. Incubation of pseudobranch cells with bafilomycin A1 (10^{-6} mol l^{-1}), a specific inhibitor of V-ATPase, reduced the rate of acid secretion by about 10% under control conditions, while no effect of bafilomycin on the rate of acid secretion of gill cells was observed. Application of amiloride (5×10^{-5} mol l^{-1}) reduced the rate of acid secretion in cells of both organs, pseudobranch and gills. Incubation of pseudobranch cells with DIDS (10^{-3} mol l^{-1}) resulted in a minor increase in the rate of proton secretion, but in cells prepared from the gills of rainbow trout acid secretion was reduced by about 30–40%. It is concluded that pseudobranch cells are equipped with various pathways to secrete protons, and that the anion exchange activity especially of pseudobranch cells appears to be different from that in gills.

Key words: pseudobranch, V-ATPase, Na^+/H^+-exchange, anion exchange, Na^+/K^+-ATPase, rainbow trout, *Oncorhynchus mykiss*, cell culture, gill cell.

Introduction

The pseudobranch is a gill-like hemibranch located within the subopercular cavity and attached to the operculum of many teleost fishes. As indicated by the term hemibranch, the gill arch supports only one row of filaments, which carry a series of gill lamellae like the filaments of the regular gill arches. In some species the lamellae are fused. The pseudobranch receives oxygenated blood from the first gill arch (Hyrtl, 1838), and in many freshwater fish is covered by the opercular epithelium, so that it can hardly have a respiratory function (Laurent and Dunel-Erb, 1984; Bridges et al., 1998). However, the innervation of the pseudobranch, including a nerve plexus located in the base of the organ and numerous non-myelinated nerve fibers ending near special pseudobranch cells, clearly implies that this organ serves a distinct physiological function.

Johannes Müller (Müller, 1839) noticed that the pseudobranch is often associated with the presence of a so-called choroid rete mirabile in the fish eye. This observation was confirmed more than a century later by Wittenberg and Haedrich (1974) and triggered the idea of a distinct functional relationship between these two organs. The choroid rete mirabile is a capillary network with a countercurrent arrangement of blood vessels (Müller, 1839; Barnett, 1951), which shows some similarity to the rete mirabile of the swimbladder, a well-known countercurrent exchanger (Kuhn et al., 1963; Pelster, 1997). The vascular arrangement is such that blood from the pseudobranch reaches the arterial section of the choroid rete, then continues to the retina before returning to the venous section of the choroid rete.

The functional significance of this puzzling arrangement is still open to speculation. In the 1960s it was observed that the P_{O_2} in the eye of teleosts with a choroid rete could reach one atmosphere, and occasionally even higher, while in fish without a choroid rete it did not exceed arterial P_{O_2} levels (Pa_{O_2}) (Wittenberg and Wittenberg, 1962, 1974; Fairbanks et al., 1969). This was recently confirmed by Waser et al. (1998). These hyperoxic P_{O_2} levels are apparently necessary to ensure oxygen supply to the avascular retina of the fish eye, because a P_{O_2} value of approximately 13 kPa, typically observed in fish blood, would not be sufficient to completely oxygenate the retina of thickness up to 500 μm (see Pelster and Randall, 1998; Pelster, 2002). Blood P_{O_2} levels exceeding Pa_{O_2} can only be explained by the presence of the Root effect, i.e. a reduction in oxygen-carrying capacity at low pH. In trout blood the Root effect is typically switched on at an extracellular pH below

approximately 7.4, and the oxygen-carrying capacity can be reduced by approximately 60% (Pelster and Weber, 1990).

A model widely used for analysis of the physiological significance of the Root effect is the fish swimbladder, and the Root effect is switched on by acid secretion of swimbladder gas gland cells. The resultant initial increase in P_{O_2} is subsequently increased by countercurrent concentration in the swimbladder rete mirabile (Kuhn et al., 1963; Pelster, 1997). If this system also occurs in the fish eye, blood must be acidified in the eye, and the resultant initial increase in P_{O_2} would subsequently be enhanced by countercurrent concentration in the choroid rete.

This basic concept of oxygen supply mechanism to the fish retina is largely accepted, but there are some important differences between the retina and the swimbladder. In the swimbladder, pH values as low as pH 6.5 have been recorded (Steen, 1963; Kobayashi et al., 1990), but the retina is very sensitive to low pH; a pH of 6.4 or the inhibition of carbonic anhydrase activity rapidly causes blindness (Maetz, 1956). Thus, in the eye the blood must be carefully acidified, sufficient to switch on the Root effect, but not so much that the retina cells are damaged. Blood leaving the retina is returned to the choroid rete where, along the partial pressure or concentration gradient, gases and also metabolites diffuse back from the venous to the arterial side and return to the retina. They are concentrated by countercurrent exchange, and the magnitude of this effect largely depends upon the magnitude of the initial increase in partial pressure or concentration, and on the properties of the countercurrent exchanger (i.e. permeability and surface area) (Kuhn et al., 1963; Pelster, 1997). If the retina generates a lot of acid to acidify the blood and switch on the Root effect (for example, enough to lower the pH from arterial levels of pH 7.8 to approximately 7.3, which is the level necessary for onset of the Root effect), a large proton gradient will be established between venous and arterial capillaries in the choroid rete, resulting in a significant countercurrent concentration of acid, and hence in severe acidification of the blood in the eye.

The pseudobranch plays a role in this situation. Experiments using isolated perfused pseudobranch preparations revealed that the blood is acidified during its passage through the tissue (Bridges et al., 1998), but the blood P_{O_2} did not increase. This suggests that the acidification was too low to switch on the Root effect. Based on these observations it was suggested that in the pseudobranch the blood is 'preconditioned' by acidification to a point just above onset of the Root effect (for example, pH 7.4–7.5). Thus, during passage through the retina, a minor additional acidification would be sufficient to liberate oxygen from hemoglobin *via* the Root effect, and the danger of overacidification would be avoided (Berenbrink, 1994; Bridges et al., 1998).

Unfortunately, there is very little information about the cellular functions of pseudobranch cells, and before this hypothesis can really be tested more background information on these cells is needed. Pseudobranch cells are hexagonal, approximately 10–15 μm wide and 6–10 μm high. The basal membrane displays membrane invaginations that form long tubules penetrating about two thirds of the cell, but never reaching the apical membrane. The filamentous mitochondria are arranged in close proximity to these tubules. Pseudobranch cells are able to secret acid, and show pentose phosphate shunt enzyme activity (Bridges et al., 1998), which is also a characteristic feature of swimbladder gas gland cells. The present study therefore set out to develop a method of isolating pseudobranch cells and elucidating what pathways for acid transfer through the cell membrane are available. Immunohistochemistry was used to characterize the cells and localize ion-transport proteins in the membrane of pseudobranch cells. Physiological experiments were also performed with gill cells, in order to identify possible differences between pseudobranch and gill cells. A histological and immunohistochemical characterization of gill cells has already been published (Goss et al., 1994; Wilson et al., 2000).

Materials and methods

Preparation of tissues

Rainbow trout *Oncorhynchus mykiss* Walbaum of approximately 25–30 cm were obtained from a local fish farm and kept in an aquarium with running tapwater at 15°C for at least 10 days prior to experimentation. Fish were anesthetized with 0.05% ethylene-glycol-monophenyl-ether (Merck) and killed by cutting the spinal chord. The gills were perfused with EDTA-PBS (in mmol l^{-1}: NaCl, 154; Na_2HPO_4, 3; KH_2PO_4, 1; EDTA, 1; glucose, 10) through the Bulbus arteriosus to remove most of the blood. The pseudobranch was dissected from the inner side of the operculum by a circular cut around the organ and pulled out using a forceps. The gills were prepared by cutting the gill arch with scissors. Both tissues were placed separately in ice-cold EDTA-PBS immediately after dissection.

Preparation of gill cells

Gill filaments were separated from the gill arches and cut into small pieces. Adhering mucus and microorganisms were removed with three consecutive washes of 10 min in PBS (composition as above, but without EDTA, to avoid premature tissue disintegration). The tissue was digested in EDTA-PBS with 0.5 g l^{-1} trypsin (T-4549; Sigma), using a modified procedure of Wood and Pärt (1997). Every 10 min, the cell suspension was collected through a 70 μm cell mesh (Becton Dickinson) in ice-cold culture medium (see below) to stop digestion. After three digestion steps, the cells were centrifuged for 5 min at 280 ***g*** (4°C). The pellet was washed with culture medium and centrifuged for a second time. Cells were resuspended in M199 (4/150; Life Technologies), supplemented with 10% fetal calf serum (FCS) and insulin–transferrin–selenium (all from Life Technologies). Culture conditions were 19°C and 0.5% CO_2. To avoid initial infections, high levels of antibiotics (100 μg ml^{-1} gentamycin; Life Technologies and 100 μg ml^{-1} kanamycin; Sigma) were used for the first culture day.

Preparation of pseudobranch cells

Connective tissue and the opercular epithelium were removed from the reddish pseudobranch tissue using a forceps. The tissue was digested in PBS (in mmol l^{-1}: NaCl, 154; Na_2HPO_4, 3; KH_2PO_4, 1; $CaCl_2$, 1.3; $MgCl_2$, 0.5; glucose, 10) with 0.5 mg ml^{-1} albumin (A-2153; Sigma), 0.22 mg ml^{-1} collagenase P (Boehringer Mannheim), 0.16 mg ml^{-1} protease I (Sigma), 0.15 mg ml^{-1} DNAse (Sigma) and 4 µl ml^{-1} elastase (Serva). Digestion was performed in a water bath at 18°C under continuous agitation. Every 10 min, the cell suspension was collected through a 70 µm cell mesh (Becton Dickinson) in sterile ice-cold culture medium (M199 + 10% FCS) to stop digestion. After three digestion steps, the cells were centrifuged for 5 min at 280 ***g***, 4°C. The pellet was washed with culture medium and centrifuged for a second time. Cells were resuspended in a modified M199 medium (see above).

As pseudobranch cells appeared to be sensitive to enzymatic digestion, in a different approach was used to isolate pseudobranch cells without digesting the tissue. The tissue was homogenized by mechanical maceration through a 70 µm nylon cell strainer (Becton Dickinson). The cells were collected in ice-cold PBS with 5% FCS to avoid re-aggregation. Cells were centrifuged for 7 min at 200 ***g*** (4°C) and the pellet was resuspended in PBS-FCS. The number of pseudobranch cells in the preparation was increased, as revealed by fluorescence microscopical studies, but physiological measurements performed with the cytosensor microphysiometer (see below) showed no apparent differences between the two preparations.

Measurement of proton release

Measurements of proton release basically followed the procedure described by Pelster (1995). Pseudobranch and gill cells were seeded into 12 mm diameter disposable polycarbonate cell capsules (Molecular Devices, Germany) at about 500 µl cell suspension per well. The number of cells incubated in the measuring chamber was variable among the preparations, because disintegration of the tissues usually resulted in isolation of cell groups or cell clusters rather than single cells, making reproducible pipetting of the cell suspension and an accurate determination of the cell number extremely difficult. Nevertheless, estimates of the cell density of the suspension were obtained by microscopic inspection using a graduated counting chamber with a volume of 0.1 µl. The cultures were incubated at 19±1°C in a humidified atmosphere of 0.5% CO_2 in air overnight. This preincubation was sufficient to ensure attachment of the cells to the membrane of the cell capsules. Because these translucent porous membranes are not suitable for microscopic examination of living cells, parallel cultures on polycarbonate culture dishes (Sarstedt) were established to control cell growth and check for bacterial infections.

Cell capsules were loaded into a cytosensor microphysiometer (Molecular Devices, Germany), in which a light-addressable potentiometric sensor (LAPS) continuously measured the rate at which the cells acidify their environment (Owicki et al., 1990; McConnell et al., 1992). The measuring chambers of the microphysiometer were intermittently perfused with a medium of low buffering capacity (0.92 mmol l^{-1} phosphate) using peristaltic pumps, to increase the sensitivity of the system. A typical pumping cycle of 120 s consisted of a flow period of 90 s, followed by a flow-off period of 30 s. Occasionally we used a pumping cycle of 180 s with a flow-off period of 90 s. During flow-off periods, protons released from the pseudobranch or gill cells accumulated in the measuring chamber and the rate of proton release was quantified by fitting the sensor data to a straight line with the least-squares procedure; the slope of this line represented the acidification rate. Numerically, a slope of 1 µV s^{-1} is close to a pH change of 0.001 pH unit min^{-1}. At the end of a measuring period, flow was resumed and the next pumping cycle began, washing out the protons that had accumulated in the previous measuring cycle. The pH change produced by the cells during a measuring cycle was typically below 0.1 pH units. The intermittent perfusion of the measuring chambers caused unattached cells to be flushed out of the measuring chamber within the first 5–10 pumping cycles.

Each measuring chamber was constantly supplied by two media (control and test); changing from one to the other was induced by an electromagnetic valve, with a time lag between valve switch and fluid arrival at the measuring chamber of approximately 3 s at a flow rate of 100 µl min^{-1}. The basic composition of the test medium was (in mmol l^{-1}): NaCl, 138; KCl, 5.0; $CaCl_2$, 0.9; $MgCl_2$, 0.5; K_2HPO_4, 0.81; KH_2PO_4, 0.11; glucose, 10, pH 7.6. For preparation of test solutions various inhibitors were added to the basic medium, carefully keeping the pH of the solution constant. Where dimethyl sulphoxide (DMSO) was necessary to solubilize a specific component, the same concentration of DMSO was also added to the control channel. The experimental temperature was 19±1°C. The pumps, valve switching and data collection were controlled by a personal computer (Macintosh) and a dedicated software package (Molecular Devices, Germany).

SDS-PAGE and western blot analysis

Protein from pseudobranch homogenate was separated by sodium dodecyl sulfate polyacrylamide-gel electrophoresis (SDS-PAGE) using the NuPage buffer system. Electrophoresis was performed with Power Ease 500, X-Cell II using NuPage 10% Bis-Tris gels (all from Novex, Germany). The SDS-PAGE was performed under reducing conditions using dithiothreitol (DTT) at a concentration of 125 µmol l^{-1}.

Electrophoretic transfer of proteins to a nitrocellulose membrane was performed using Power Ease 500 (Novex, Germany). The transfer was conducted for 1 h at a constant voltage of 25 V (160 mA). The nitrocellulose membranes were placed in a sealed bag containing 10% BSA, 10% FCS and 0.1% Tween-20 (Sigma) in 100 mmol l^{-1} phosphate buffer and gently agitated for 1.5 h at room temperature (22–24°C). After washing, the membranes were incubated overnight at 4°C with a chicken Na^+/K^+-ATPase antibody (Biogenesis, UK) diluted

1:50 000 in phosphate buffer containing 1% BSA, 1% FCS and 0.1% Tween-20. The membranes then were washed and incubated for 1 h with Sigma anti-chicken IgG (A9046) diluted 1:10 000 and conjugated with horseradish peroxidase (HRP) in phosphate buffer, with 1% BSA, 1% FCS and 0.1% Tween-20 at room temperature. Antibody binding was visualized by enhanced chemiluminescence (ECL; Amersham Life Science).

For western blot analysis to demonstrate the presence of V-ATPase, proteins were electrophoretically separated under reducing conditions as described above and blotted onto PVDF-membranes (BioRad, CA, USA) using a constant voltage of 25 V (160 mA) for 1 h. Membranes were blocked for 1 h with 7% BSA (Sigma) and 7% FCS (Life Technologies, Austria) and 0.1% Tween-20 (Sigma) in 0.1 mol l^{-1} PBS at room temperature. Primary antibodies directed against the B subunit of V-ATPase were obtained by generating an artificial peptide based on the cDNA sequence information (Niederstätter and Pelster, 2000) and immunization of rabbits (S. T. Bösch, H, Niederstätter and B. Pelster, submitted for publication). Primary antibody incubation was performed overnight at 4°C in blocking buffer. After additional washing steps the membranes were probed for 1 h with an HRP-conjugated second antibody (HRP-conjugated anti-rabbit IgG; Sigma). Finally proteins were visualized using the enhanced chemiluminescence (ECL) detection reagents (Amersham, UK).

For western blot analysis to demonstrate the presence of anion exchanger, proteins were separated and blotted to a PDF membrane as described above, and commercially available antibodies (Rabbit Anti-rat AE21-A; Alpha Diagnostics International) against anion exchanger 2 were used. Primary antibody incubation was performed overnight at 4°C in blocking buffer. After additional washing steps the membranes were probed for 1 h with an HRP-conjugated second antibody (HRP-conjugated anti-rabbit IgG, Sigma). Finally, proteins were visualized using the enhanced chemiluminescence (ECL) detection reagents (Amersham, UK).

Fluorescence labeling of cultured cells

The pseudobranch cells were seeded on permeable supports, as for the Cytosensor experiments. To speed up cell adherence, medium was removed from the underside of the permeable membrane, so that the lowering of the fluid level forced contact of the cells with the support. After 15 min at 4°C, the adherent cells were washed twice in PBS. Normally, cells were put into ice-cold 4% paraformaldehyde (PFA) immediately afterwards. For *in vivo* mitochondrial staining, cells were incubated in Mito Tracker Orange (Molecular Probes, Oregon, USA) at 500 nmol l^{-1} for 30 min in PBS before fixation.

Fixation was performed at 4°C overnight. The cells were then permeabilized with 0.05% SDS (Merck) and 0.1% Tween-20 (Sigma) for 15 min and blocked with 1% BSA (Sigma) in PBS for 15 min at room temperature. At least three consecutive washes with PBS were performed between all steps of the fixing and staining procedure.

Mitochondria

In fixed cells, mitochondria were stained by labeling the endogenous mitochondrial biotin with Streptavidin-FITC (Dako, DK, USA) at 1:50 dilution in PBS for 30 min (Ruggiero and Sheffield, 1998).

Cytokeratin

The antibody (M 3515 monoclonal mouse anti-human cytokeratins, AE1/AE3; Dako) was diluted 1:100 in PBS with 1% BSA and incubated for 1 h at room temperature. Secondary antibody (rabbit anti-mouse TRITC R0270; Dako) was applied at a dilution of 1:100 in PBS.

Na^+/K^+-ATPase

For antibody-labeling of the Na^+/K^+-ATPase, permeabilization was omitted. Chicken Na^+/K^+-ATPase antibody (Biogenesis, UK) was applied at a dilution of 1:100 in PBS with 1% BSA for 1 h at room temperature. After washing, the samples were incubated for 1 h with Sigma anti-chicken IgG (A9046) fluorescein isothiocyanate (FITC)-conjugated antibody, diluted 1:100 in PBS.

Stained cells were washed in PBS and embedded in Vectashield H-1000 mounting medium (Vector Laboratories, CA, USA). Analysis was performed with a laser-scanning microscope (Zeiss, LSM 510) at 64× magnification. For optimum resolution, confocal picture stacks were deconvoluted using Huygens software (SVI, NL, USA) using *Maximum Likelihood Estimation* algorithm.

Immunohistochemistry on tissue sections

After dissection, the pseudobranch was fixed in 4% PFA at 4°C overnight. The tissue was washed in PBS (3× 30 min) and dehydrated in a series of ethanol baths (30 min each in 70%, 80% and 90% ethanol, 3× 1 h in 100% ethanol). Prior to the final embedding in paraffin, dehydrated samples were incubated in methyl benzoate (1× overnight, 3× 3–12 h), benzol (2× 30 min), benzol/paraffin (1× 2 h at 60°C) and three changes in paraffin (each 12–16 h).

Sections 4–5 μm thick were cut on a Reichert–Jung microtome and deparaffinized. Slices were prepared for antibody staining by antigen retrieval with proteinase-K digestion. Acetylation was performed with 0.5% acetic acid anhydride in 0.1 mol l^{-1} Tris-HCl, pH 8.0. Unspecific binding was blocked with 10% FCS in TBS.

For the immunocytochemical localization of V-ATPase, primary antibodies directed against subunit B (see above) were used. Incubation with the primary antibody at a dilution of 1:350 in blocking buffer was undertaken at 4°C overnight. After five washes with TBS, cells were incubated with a polyclonal biotinylated anti-rabbit/mouse IgG (Duett-ABC Kit Solution C; Dako, DK, USA) for 20 min. Then additional washes were performed and the cells were probed with an anti-biotin alkaline-phosphatase antibody (diluted 1:100; Dako) for 1 h.

Similarly, cells were incubated with the primary antibody directed against anion exchanger 2 (Rabbit Anti-rat AE21-A, Alpha Diagnostics International, TX, USA) at a dilution of

1:250 in blocking buffer overnight. Secondary antibodies were visualized with a solution of 4-nitroblue tetrasodium chloride (Roche Molecular Biochemicals) and 5-bromo-4-chloro-3-indolylphosphate-4-toluisin salt (Roche Molecular Biochemicals), as a purple stain. Pictures were recorded using a digital camera (Nikon Coolpix 990) on a bright-field light microscope (Reichert Polyvar). Images were processed in Photoshop software (Adobe) to optimize brightness and contrast. Special care was taken to keep recording conditions and imaging parameters constant within probe and control samples.

Data analysis and statistics

The rate of acid release (acidification rate in $\mu V\,s^{-1}$) was quantified by fitting the sensor data collected during periods of interrupted flow to a straight line using the least-squares procedure. To reduce data scatter induced by the variable acidification rate measured under control conditions (see above) the data were also normalized by setting the acidification rate recorded during a 4–8 min period before the administration of a drug to 100%. Normalized data are presented as percentage of basal rate (control rate). Data are given as means ± S.E.M. Statistical differences from control or between treatments were tested by analysis of variance (ANOVA), followed by a multiple-comparison procedure (SigmaStat) or, where applicable, the Student's *t*-test. Significance of differences was accepted when $P<0.05$.

Results

The pseudobranch consists of several cell types, including flat epithelial cells, pillar cells and the pseudobranch cells. Cell suspensions prepared by Ca^{2+} depletion and mechanical maceration contained a distinct population of cells, which always kept their relatively flat shape and did not round up in suspension or proliferate after adhering to the surface (Fig. 1).

Pseudobranch cells are epithelial cells, which typically are characterized by the presence of epithelial cytokeratins. Using antibodies directed against cytokeratins, cells fixed immediately after isolation could be clustered into three groups. The most intense fluorescence signal was observed in small, spheroid cells of rather undifferentiated character (Fig. 2A,B). The second group consisted of a small population of an intermediate cell type, which showed the typical mitochondrial arrangement of pseudobranch cells, but were smaller and more spheroid, and stained positive for cytokeratins (Fig. 2C). The third group were apparently fully differentiated, mitochondria-rich cells (Fig. 2C,D), of which a small fraction reacted weakly positive for cytokeratins (Fig. 2D), but most did not react at all with this antibody (Fig. 2C). Microscopical inspection of these cells over 3–4 days revealed no evidence of any further differentiation or proliferation of any cell type.

Fluorescence microscopical characterization of the cells revealed the presence of a large number of mitochondria.

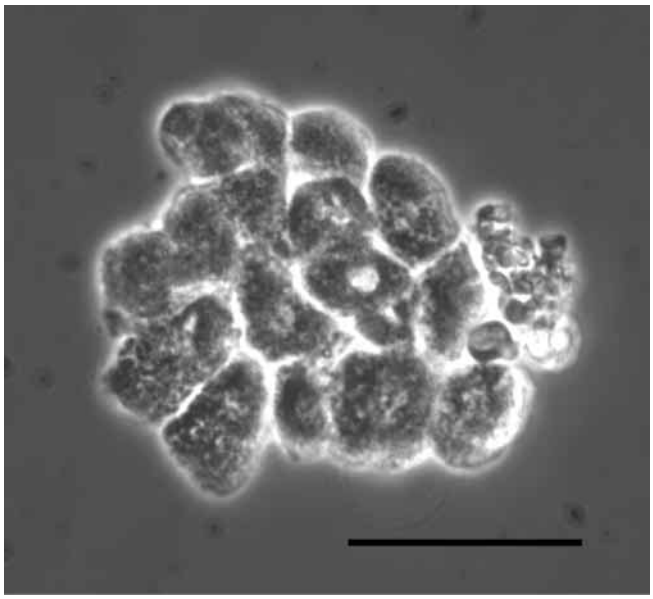

Fig. 1. A cluster of adhesive mitochondria-rich cells isolated from the pseudobranch. Scale bar, 50 μm.

Incubation of fixed cells with FITC-labeled streptavidin revealed a staining pattern (Fig. 3) that was quite photostable, similar to the results obtained with *in vivo* staining using the mitochondria-selective dyes Mitotracker green FM and Mitotracker orange.

Using a commercially available antibody directed against anion-exchanger 2, we attempted to localize the anion exchanger in pseudobranch cells. Fig. 4 shows that a positive immunohistochemical reaction was observed in the membranes of almost all cells. Specificity of the antibody was tested by western blot analysis. Several bands were identified, the most prominent at approximately 40 kDa, with a fainter double band at approximately 60 kDa (Fig. 5B).

To demonstrate the presence of Na^+/K^+-ATPase, cultured pseudobranch cells were incubated with a commercially available chicken anti-canine antibody. Confocal microscopy revealed extensive binding of the antibody to proteins of the basal membrane invaginations (Fig. 6). Specificity of the antibody was checked by western blot analysis. A double band was always observed at a molecular mass of approximately 30–35 kDa, and an additional band was present with a molecular mass of about 45 kDA (Fig. 5A).

A specific antibody directed against a conserved sequence between amino acids 67 and 75 of the B subunit of V-ATPase was used to search for the expression of V-ATPase in pseudobranch cells. A positive staining reaction was found in the membranes of most cells, especially in the tubular membranes (Fig. 7A). Controls without primary antibody showed no staining reaction (Fig. 7B). Western blot analysis resulted in a single band of molecular mass slightly above 50 kDa (Fig. 5C), which corresponds to the molecular mass of subunit B.

The rate of proton secretion of cells prepared from the

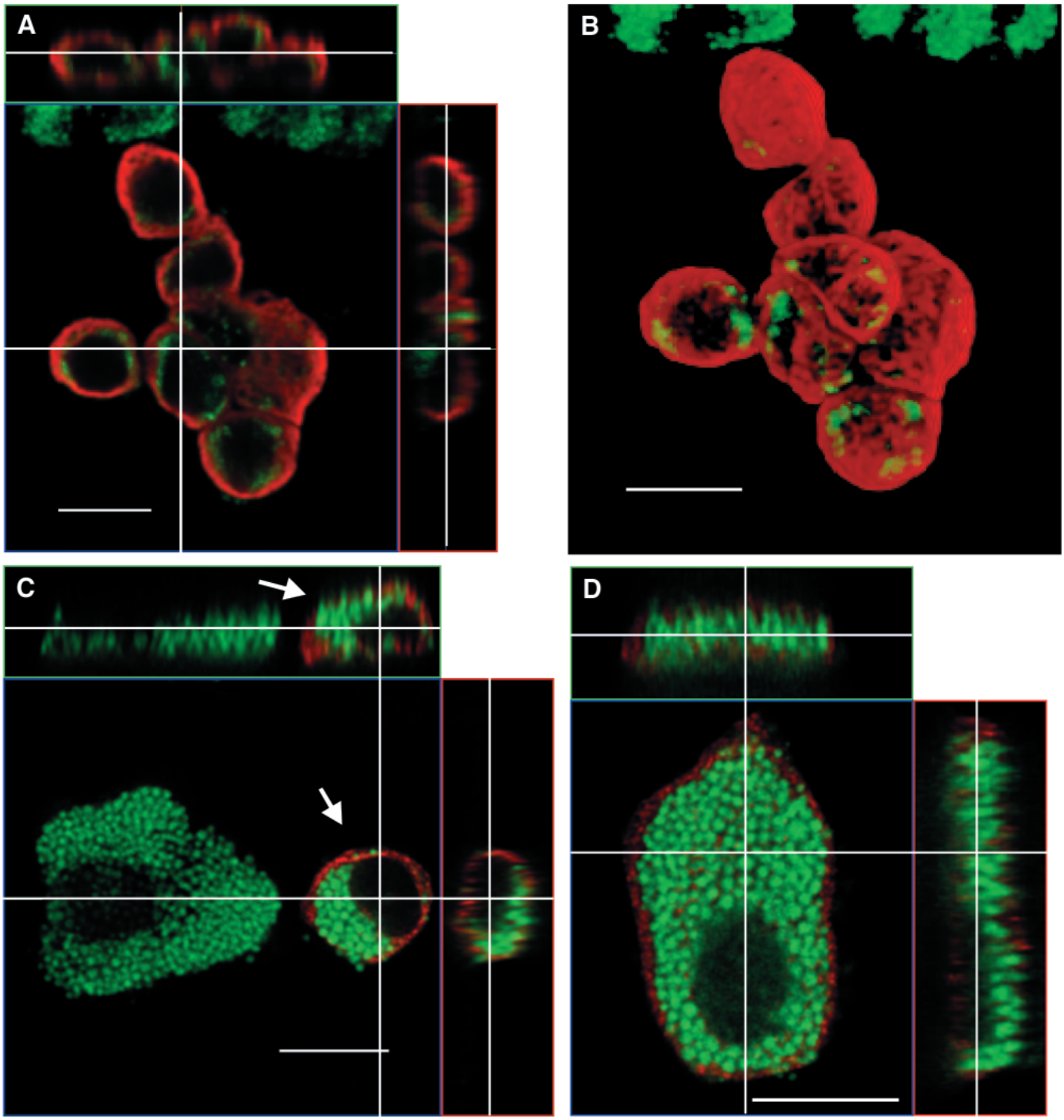

Fig. 2. Immunohistochemical localization of cytokeratin (red signal) in freshly prepared pseudobranch cells. FITC-labeled streptavidin was used to stain mitochondria (green signal). Three groups of cells were identified. The most intense staining was observed in small and largely undifferentiated cells (A,B). (A) Confocal images with three optical sections of the cells. The top image shows a *x,z* section, bottom left a *x,y* section, and bottom right a *y,z* section. Within each image the locations of the two accompanying sections are indicated by white cross-sectional bars, i.e. in the *x,y* section (bottom left) the horizontal bar indicates the location of the *x,z* section (top image), and the vertical bar the location of the *y,z* section (bottom right). (B) A three-dimensional reconstruction. (C) Cells from a small population of intermediate cell type, with the typical mitochondrial arrangement of pseudobranch cells, but smaller and more spheroid. These cells also stained positive for cytokeratins (cell marked with an arrow in C), but the staining was not as intense as in the undifferentiated cells. Apparently fully differentiated mitochondria-rich cells showed a very weak or no positive reaction. (D) A fully differentiated cell with a faint cytokeratin staining was observed. The staining only became visible at very high amplification of the red channel. In C and D, confocal images are shown with three optical sections of the cells. The top image shows a *x,z* section, bottom left a *x,y* section, and bottom right a *y,z* section. The locations of the sections within the cell cluster are indicated by white cross-sectional bars (see explanation to A). Scale bars, 10 μm.

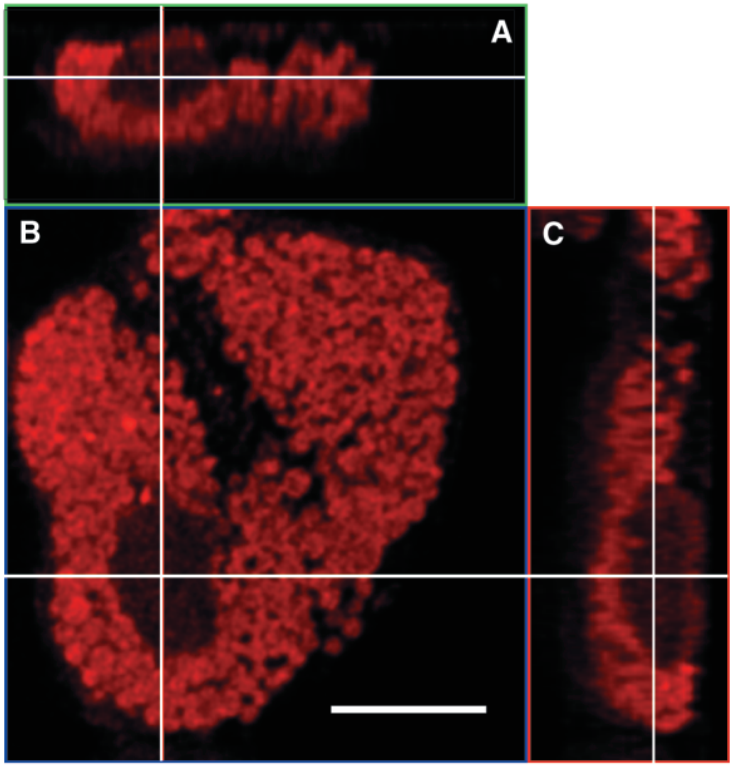

Fig. 3. Incubating fixed pseudobranch cells with FITC-labeled streptavidin resulted in a photostable staining of mitochondria. The confocal image shows three optical sections of a pseudobranch cell in the *x,z* (A), *x,y* (B) and *y,z* (C) planes. Within each image the locations of the two accompanying sections are indicated by white cross-sectional bars, i.e. in the *x,y* section (bottom left) the horizontal bar indicates the location of the *x,z* section (top image), and the vertical bar the location of the *y,z* section (bottom right). A similar picture was obtained by *in vivo* staining using the mitochondria-selective dyes Mitotracker green FM and Mitotracker orange. Scale bar, 10 μm.

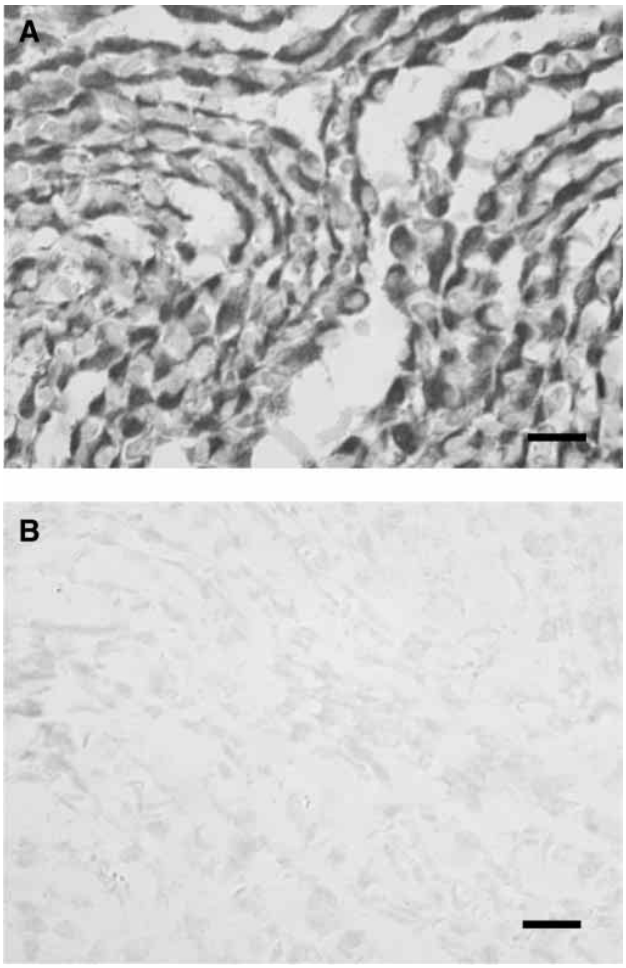

Fig. 4. Immunocytochemical staining of the anion-exchanger 2 in pseudobranch cells. An antibody (rabbit anti rat AE2) directed against a specific 21-amino-acid peptide from rat showed cross-reactivity in pseudobranch tissue (A). Control sections with the primary antibody omitted showed no staining (B). Scale bars, 20 μm.

pseudobranch and from gills was measured using a cytosensor microphysiometer. Cells seeded into the cell capsules did attach to the collagen-coated polycarbonate membrane, and the acid secretion of these attached cells could be measured without additional immobilization. In the measuring chamber the activity of the cells was very stable and could be measured for many hours. The acidification rate of the external medium was typically 10–50 $\mu V\,s^{-1}$. For pseudobranch cells, the mean acidification rate of the external medium was $26.21\pm2.25\,\mu V\,s^{-1}$ for four preparations, and the cell density of the suspension seeded into the capsule caps was $0.123\pm0.021\times10^5$ cells ml^{-1} (see Materials and methods). The average rate of acid secretion of gill cells was $16.53\pm0.22\,\mu V\,s^{-1}$ (N=4), with the suspension seeded into the capsule caps at a cell density of $2.98\pm1.28\times10^5$ cells ml^{-1}.

In pseudobranch cells as well as in gill cells the secretion of protons was diminished in the presence of amiloride, an inhibitor of Na^+/H^+-exchange (Fig. 8A,B). In pseudobranch cells, substitution of Na^+ in the basic medium by trimethylamine (TMA) caused a 10–15% decrease in the rate of acid secretion, which is in line with the effect of amiloride. Similarly, incubation of pseudobranch cells with bafilomycin A1, a specific inhibitor of V-ATPase, resulted in a decrease in proton secretion of approximately 10% (Fig. 9A). In gill cells, however, bafilomycin had no effect on the rate of acid secretion (Fig. 9B). 4,4-diisothiocyanostilbene-2,2-disulfonic acid (DIDS) (10^{-3} mol l^{-1}), an inhibitor of Cl^-/HCO_3^- exchange, caused a minor but significant increase in the rate of proton release in pseudobranch cells (Fig. 10A). At a concentration of 5×10^{-4} mol l^{-1} the observed increase in proton secretion was not significant. Replacing chloride in the basic medium either by gluconate or by nitrate caused a transient increase in the rate of acid secretion, which is in line with the effect observed in the presence of DIDS. In gill cells of rainbow trout, DIDS at a concentration of 5×10^{-4} mol l^{-1} caused a 30–40% reduction in the rate of proton secretion (Fig. 10B).

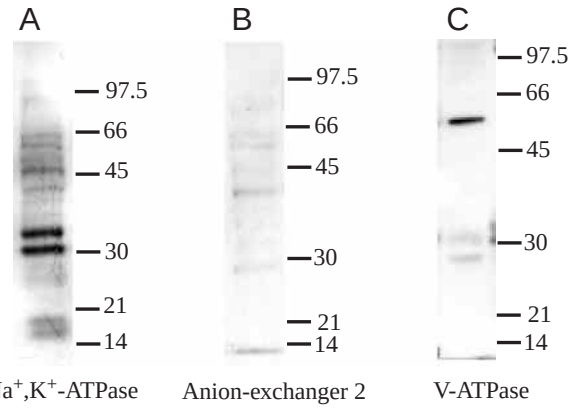

Fig. 5. Western-blot analysis of Na^+/K^+-ATPase (A), anion-exchanger 2 (B) and vacuolar-type ATPase (C) in pseudobranch tissue. The positions of molecular mass markers (kDa) are shown.

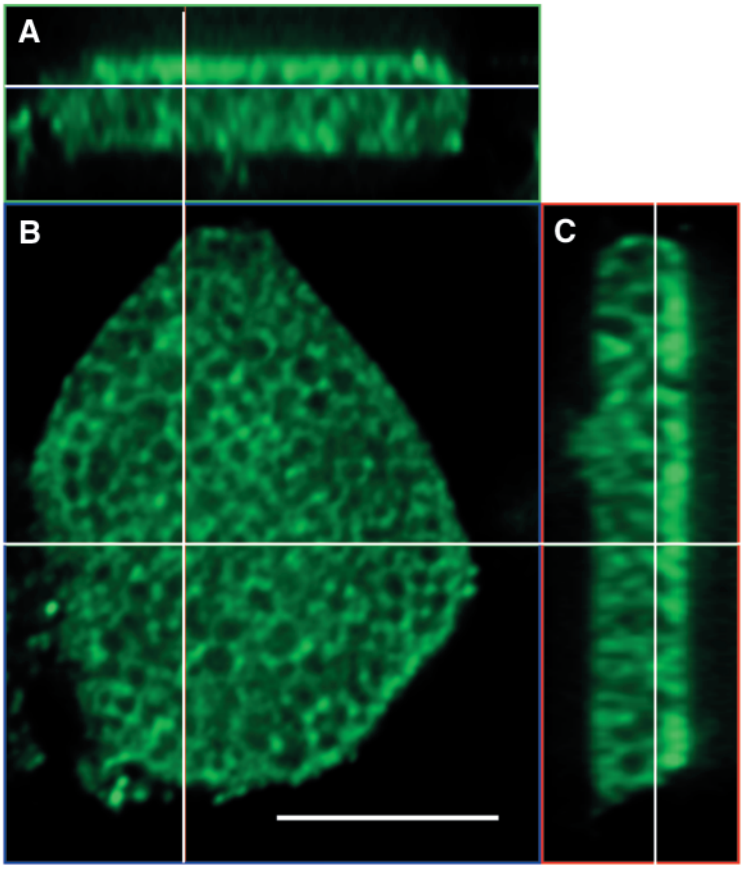

Fig. 6. Immunohistochemical localization of Na^+/K^+-ATPase in pseudobranch cells. The confocal image shows three optical sections of a pseudobranch cell in the (A) *x,z*, (B) the *x,y* and (C) the *y,z* planes. Within each image the location of the two accompanying sections is indicated by white cross-sectional bars, i.e. in the *x,y* section (bottom left) the horizontal bar indicates the location of the *x,z* section (top image), and the vertical bar the location of the *y,z* section (bottom right). Note that Na^+/K^+-ATPase immunoreactivity is located at all cell membranes. Scale bar, 10 μm.

Discussion

The pseudobranch comprises several cell types. The lamellae are vascularized by pillar capillaries similar to the regular gill lamellae, and thus the pseudobranch includes pillar cells as well as pavement cells. The pseudobranch, however, is mainly characterized by the presence of a special cell type that is not found in gills, the pseudobranch cells (Laurent and Dunel-Erb, 1984). The pseudobranch cell shows some characteristics typical of chloride cells, such as the presence of large numbers of mitochondria. They do not, however, have the typical apical pits of chloride cells, or at least these pits have no contact with the external water. The results of our study clearly show that these pseudobranch cells can be isolated and cultured. Using mechanical maceration and a Ca^{2+}-free environment we were able to isolate a distinct population of mitochondria-rich cells that always kept their relatively cuboidal shape and did not round up in suspension or proliferate after adhering to the surface of a culture dish. The histological appearance showed similarities to pseudobranch cells. Furthermore, our immunocytochemical analysis revealed the presence of an extensive tubular system at the basal side. Using a commercially available antibody to localize Na^+/K^+-ATPase within these cells a positive staining reaction was observed within the cell membranes, and western blot analysis yielded bands corresponding to the molecular mass of the unglycosylated or partially glycosylated β-subunit of Na^+/K^+-ATPase (Mobasheri et al., 2000). This suggests that the immunoreactivity is due to the presence of Na^+/K^+-ATPase in the membranes of these cells. These features match our current conception of pseudobranch cells (Laurent and Dunel-Erb, 1984; Dendy et al., 1973). We therefore conclude that the cells isolated from this organ were mainly pseudobranch cells, and not pavement cells, which typically are isolated from gills (Pärt et al., 1993; Pärt and Bergström, 1995; Wood and Pärt, 1997; Gilmour et al., 1998; Kelly et al., 1999). A recent study, however, reported successful isolation of mitochondria-rich cells from trout gills, with clear similarities to chloride cells (Fletcher et al., 2000).

Despite their complex morphology, pseudobranch cells are clearly of epithelial origin. Therefore it was surprising that most of the fully differentiated cells showed no positive staining for the epithelial marker cytokeratin, and even in those cells where a positive antibody reaction was observed, it could only be visualized using very high signal amplification. On the other hand, a fraction of small, undifferentiated cells in our preparations was nicely stained by the antibody directed against epithelial cytokeratins. In addition, a small population of cells, which exhibited both a strong fluorescence signal (indicating the presence of cytokeratin) and a high density of mitochondria, was present. These cells may be in a transitional differentiation state, with mitochondria already present

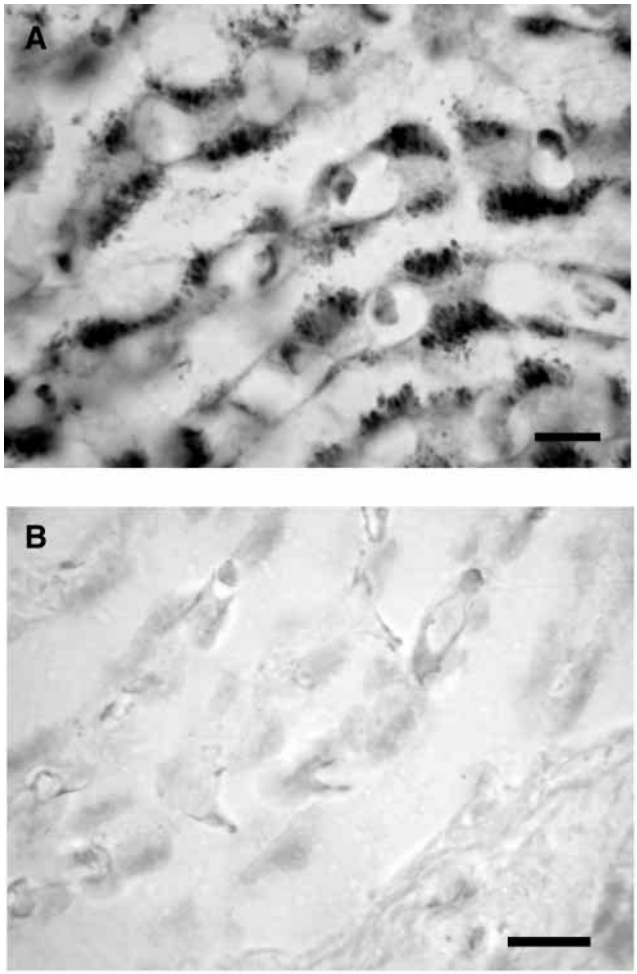

Fig. 7. Immunohistochemical staining of subunit B of vacuolar-type ATPase using an antibody directed against a conserved region of the protein (A). A positive staining reaction was found in the membranes of most cells, especially in the tubular region. Control sections incubated without the primary antibody showed no staining at all (B). Scale bar, 10 μm.

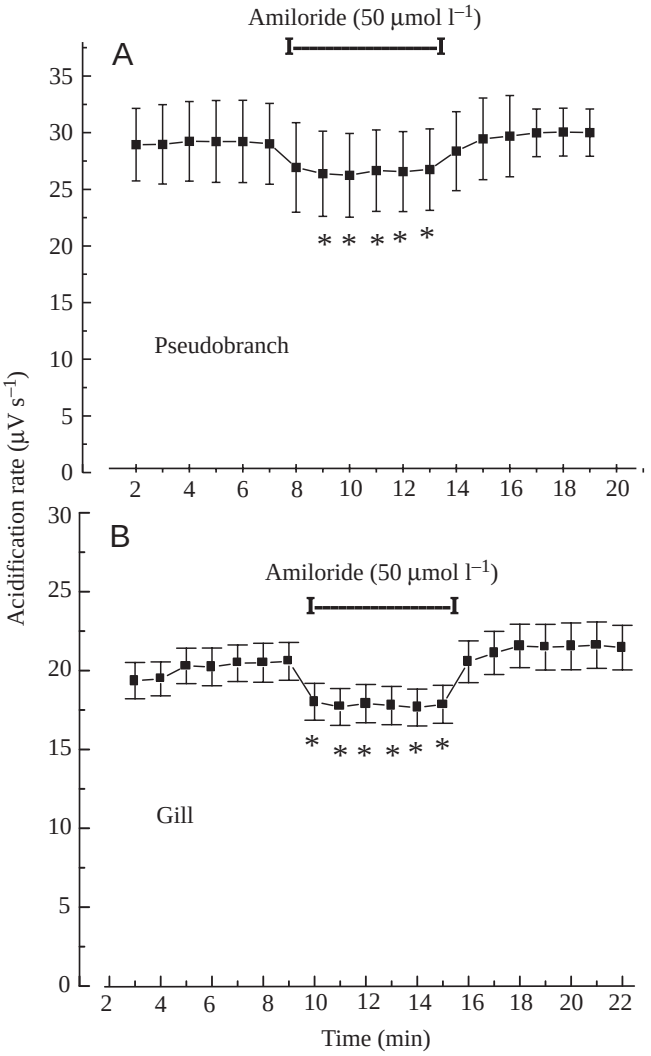

Fig. 8. The effect of amiloride, an inhibitor of Na^+/H^+-exchange, on the rate of acidification of the external medium induced by acid secretion of isolated pseudobranch cells (A) and gill cells (B) as a function of time. Amiloride (50 μmol l^{-1}) was added for the period indicated. Values are means ± S.E.M., *N*=12 (A); *N*=7 (B). Asterisks indicate significant differences from values before application of amiloride.

but the tubular system not yet established. This idea is further supported by the nucleus-to-cytoplasm volume ratio, which in these cells was smaller than in the obviously undifferentiated cells, but higher than in the fully differentiated pseudobranch cells. If these three different cell populations do indeed represent different states of differentiation, our observations suggest that pseudobranch cells abandon the expression of epithelial cytokeratin during differentiation. It may also be possible that the cells switch to different cytokeratins that are not recognized by the antibody used in our experiments. This explanation is unlikely, however, because the antibody is known to recognize a large variety of different cytokeratins. Unfortunately, even after 4 days in primary culture, no further differentiation of any of these cell types was observed. On the other hand, nor did we observe any proliferation of the pseudobranch cells. This lack of proliferation in culture, however, might reflect an inability to differentiate, so that this observation does not necessarily refute the idea that the different cell populations may represent various states of pseudobranch cell differentiation.

According to the hypothesis that pseudobranch cells are able to titrate blood pH down a level just above the threshold for the onset of the Root effect (Berenbrink, 1994; Bridges et al., 1998), acid must be secreted from this organ. The pseudobranch comprises several cell types, most of which are also typical of teleost gills. The only cell type that is unique to the pseudobranch is the so-called pseudobranch cell (Laurent and Dunel-Erb, 1984). It therefore is quite likely that this cell type is somehow related to the special function of this organ. Our attempts to identify acid-secreting pathways in these cells revealed the presence of an anion exchanger, Na^+/H^+-exchange and a V-ATPase.

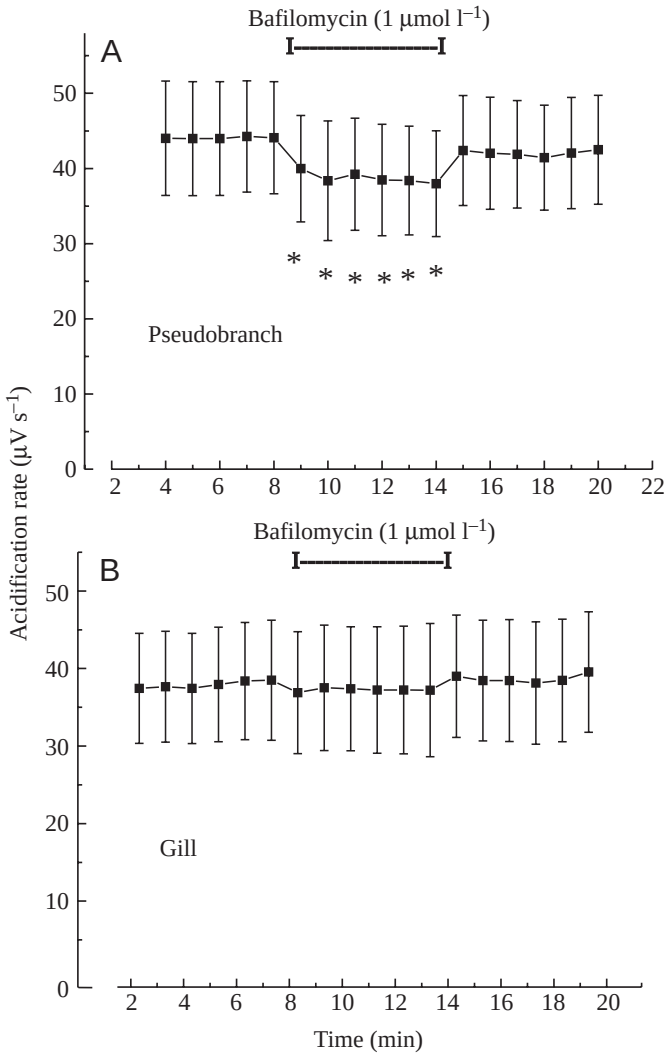

Fig. 9. The effect of bafilomycin, an inhibitor of V-ATPase, on the rate of acidification of the external medium induced by acid secretion of isolated pseudobranch cells (A) and gill cells (B) as a function of time. Bafilomycin (1 μmol l^{-1}) was added for the period indicated. Values are means ± S.E.M., *N*=8 (A); *N*=9 (B). Asterisks indicate significant differences from the values before application of bafilomycin.

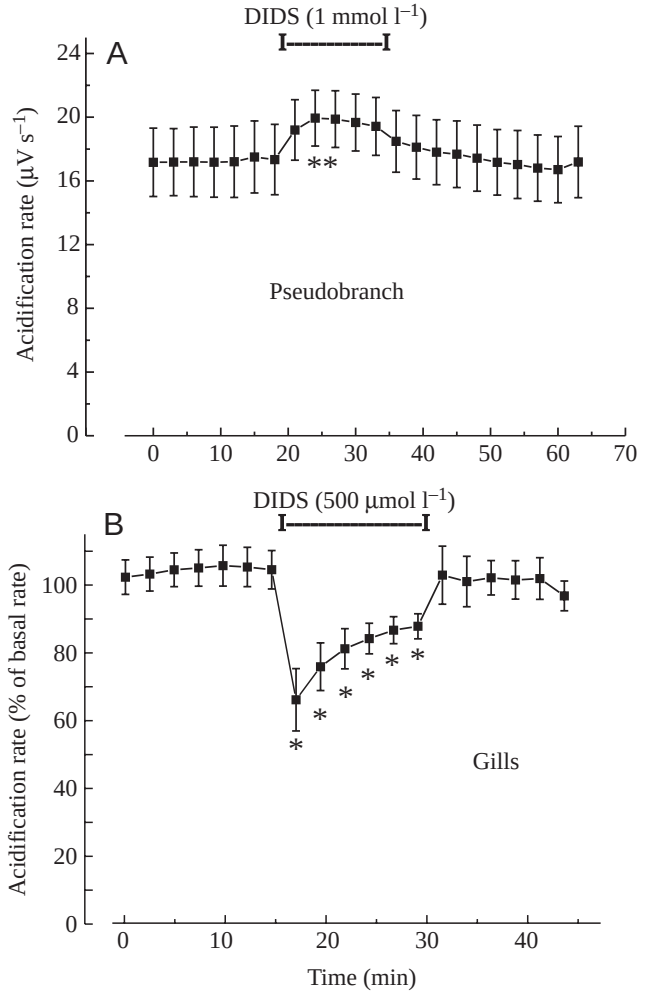

Fig. 10. The effect of DIDS, an inhibitor of anion exchange, on the rate of acidification of the external medium induced by acid secretion of isolated pseudobranch cells (A) and gill cells (B) as a function of time. DIDS (1 mmol l^{-1} in pseudobranch cells and 500 μmol l^{-1} in gill cells) was added for the period indicated. Values are means ± S.E.M., *N*=9 (A); *N*=11 (B). Asterisks indicate significant differences from values before application of DIDS.

Immunohistochemistry using a commercially available antibody directed against mammalian anion-exchanger 2 resulted in a very strong signal in the cell membranes of the pseudobranch cells, including the tubular system. Western blot analysis to test the specificity of the antibody resulted in several bands, the molecular mass of the main ones being 40 and 60 kDa. Although the mammalian protein has a molecular mass of approximately 100 kDa, fragments of 40 and 60 kDa have been observed in western blots (Wagner et al., 1987). Furthermore, the anion exchange-inhibitor DIDS and the anion-exchange protein apparently produced a highly autofluorescent complex, because cultured cells incubated with DIDS produced highly fluorescent cells, and the distribution of this fluorescence signal was very similar to the result obtained with the antibody directed against the anion exchanger alone. Thus, we conclude that the antibody binds to an anion-exchanger-like protein in pseudobranch cells. Problems with autofluorescence and the structure of the pseudobranch cells, consisting mainly of membranes (i.e. the tubular system) and mitochondria with very little free cytoplasm, made reproducible measurements of intracellular pH using fluorescent dyes almost impossible.

Although these histological data show the existence of an anion exchanger in the tubular system of pseudobranch cells, inhibition of this exchanger only caused a minor increase in acid transfer across the cell membranes. This is in contrast to gill cells, in which inhibition of anion exchange caused a significant reduction in acid release. Testing the influence of HCO_3^--buffered medium on the regulation of intracellular pH in cultured gill cells of rainbow trout, Wood and Pärt (2000)

concluded that these cells use Na^+-dependent anion exchange, and that Na^+-independent anion exchange was absent under isotonic conditions. This is in agreement with our results. The Na^+-dependent anion exchanger uses the Na^+ gradient to bring HCO_3^- into the cell. Inhibition of this exchanger increases the HCO_3^- concentration, and thus the buffer capacity, in the extracellular fluid, resulting in an apparent reduction in the rate of acid secretion measured by the cytosensor microphysiometer, which has also been shown for swimbladder gas gland cells (Pelster, 1995). Sodium independent Cl^-/HCO_3^- exchange, in turn, is regulated by the internal pH and usually extrudes base under physiological conditions. In consequence, inhibition of this exchanger causes an increase in the apparent rate of acid secretion. The obvious conclusion from these results, therefore, is that pseudobranch cells, in contrast to gill cells, use sodium independent Cl^-/HCO_3^- exchange, and under control conditions this exchanger contributes to the removal of HCO_3^- from the cell.

Application of amiloride induced a minor but significant reduction in the rate of acid secretion, suggesting that Na^+/H^+ exchange is present and contributes to acid secretion by pseudobranch cells. The same was observed for gill cells. Na^+/H^+ exchange appears to be present in most cells and uses the sodium gradient as a driving force to remove protons from the cell (Harvey and Ehrenfeld, 1988; Kramhoft et al., 1988). Its presence in gill cells is also well established (Wood and Pärt, 2000).

A third mechanism for transporting protons across the cell membrane is a proton pump, a V-ATPase. The importance of V-ATPase for the uptake of sodium by gill cells of freshwater fish is well established in several species of adult fish (Perry et al., 2000; Wilson et al., 2000), and a new model proposes that Na^+ uptake occurs passively *via* apical Na^+ conductance channels, the uptake being energized by a membrane-bound V-ATPase located in the apical membranes of gill cells (Perry, 1997; Fenwick et al., 1999). Several studies have located V-ATPase in apical membranes of gill cells (Lin et al., 1994; Laurent et al., 1994; Goss et al., 1994; Lin and Randall, 1995; Sullivan et al., 1996), although it remains controversial whether this ATPase is located in pavement cells, and/or chloride cells. Our results suggest that this V-ATPase is not involved in acid–base regulation in cultured gill cells under isosmotic conditions, which confirms the results of Wood and Pärt (2000). In cultured pseudobranch cells, however, we observed a minor but significant decrease in the rate of acid secretion after application of bafilomycin A1, and demonstrated the presence of this protein in cell membranes by immunohistochemistry. Our results therefore establish the expression of V-ATPase in pseudobranch cells, and suggest that this ATPase is involved in acid–base regulation under isosmotic conditions.

Although these pharmacological and immunhistochemical data clearly show that an anion exchanger, Na^+/H^+ exchange and V-ATPase are present in pseudobranch cells, inhibition of each single pathway caused only a minor change in the rate of acid secretion of these cells. So what can be the major pathway to transfer acid equivalents from the cytoplasm to the extracellular space? There is no immediate and clear answer to this question. It is well established that if redundant pathways are present, selective inhibition of one of these pathways may result in an increase in the activity of the other pathways. Therefore, in our experiments, inhibition of Na^+/H^+ exchange, for example, may have stimulated V-ATPase or *vice versa*. It has also been shown for gas gland cells, for example, that the activity of the various pathways is not constant, but varies with extracellular pH (Sötz et al., 2002). Another important aspect is aerobic metabolism. As demonstrated by Owicki and Parce (1992), glucose oxidation results in the production of 0.167 protons per ATP molecule produced. Thus, aerobic metabolism results in an acidification of the cell, and also in the production of CO_2, which leaves the cell by diffusion. An increase in extracellular P_{CO_2} shifts the equilibrium of the CO_2/HCO_3^- towards the formation of HCO_3^-, and thereby is equivalent to an extrusion of acid. Pseudobranch cells are virtually packed with mitochondria, and our result suggests therefore that aerobic metabolism and diffusion of CO_2 significantly contribute to the acid production and acid release of these cells.

In summary, the results of our study show that pseudobranch cells can be taken into primary culture, and these cultured cells may serve as a very useful model for the analysis of ion transport characteristics and metabolic control. Immunohistochemistry and physiological experiments show that pseudobranch cells are equipped with various mechanisms for the transfer of protons through the cell membrane. In cultured gill pavement cells a sodium-dependent anion exchange appears to contribute to acid release and control of intracellular pH, but in pseudobranch cells a Na^+-independent anion exchange was observed. In addition, V-ATPase, which is present in both cell types, is involved in acid–base regulation under isosmotic conditions in pseudobranch cells, which in gill cells is not the case. In evolutionary terms, the differentiation of the pseudobranch at the site of the hyoid arch and of the holobranchs on each of the branchial arches therefore produced morphologically as well as physiologically different organs. With respect to the possible function of the pseudobranch, our results show that the rate of acid secretion of pseudobranch cells is higher than in gill epithelial cells, which is consistent with the idea that, in the pseudobranch, the blood is ‘preconditioned’ by acidification to reduce the amount of acid that must be secreted by retina cells in order to switch on the Root effect.

The study was financially supported by the Fonds zur Förderung der wissenschaftlichen Forschung (FWF, P14174-BIO).

References

Barnett, C. H. (1951). The structure and function of the choroidal gland of teleostean fish. *J. Anat.* **85**, 113-119.

Berenbrink, M. (1994). Die Kontrolle des intrazellulären pH in den

Erythrozyten von Knochenfischen. Dissertation, Math.-Nat. Fakultät Universität Düsseldorf: Verlag Shaker.

Bridges, C. R., Berenbrink, M., Müller, R. and Waser, W. (1998). Physiology and biochemistry of the pseudobranch: An unanswered question? *Comp. Biochem. Physiol*. **119A**, 67-77.

Dendy, L. A., Philpott, C. W. and Deter, R. L. (1973). Localization of Na^+, K^+-ATPase and other enzymes in teleost pseudobranch II. Morphological characterization of intact pseudobranch, subcellular fractions, and plasma membrane substructure. *J. Cell Biol*. **57**, 689-703.

Fairbanks, M. B., Hoffert, J. R. and Fromm, P. O. (1969). The dependence of the oxygen-concentrating mechanism of the teleost eye (*Salmo gairdneri*) on the enzyme carbonic anhydrase. *J. Gen. Physiol*. **54**, 203-211.

Fenwick, J. C., Bonga, S. E. W. and Flik, G. (1999). *In vivo* bafilomycin-sensitive Na^+ uptake in young freshwater fish. *J. Exp. Biol*. **202**, 3659-3666.

Fletcher, M., Kelly, S. P., Pärt, P., ODonnell, M. J. and Wood, C. M. (2000). Transport properties of cultured branchial epithelia from freshwater rainbow trout: A novel preparation with mitochondria-rich cells. *J. Exp. Biol*. **203**, 1523-1537.

Gilmour, K. M., Pärt, P., Prunet, P., Pisam, M., McDonald, D. G. and Wood, C. M. (1998). Permeability and morphology of a cultured branchial epithelium from the rainbow trout during prolonged apical exposure to fresh water. *J. Exp. Zool*. **281**, 531-545.

Goss, G. G., Wood, C. M., Laurent, P. and Perry, S. F. (1994). Morphological responses of the rainbow trout (*Oncorhynchus mykiss*) gill to hyperoxia, base ($NaHCO_3$) and acid (HCl) infusions. *Fish Physiol. Biochem*. **12**, 465-477.

Harvey, B. J. and Ehrenfeld, J. (1988). Role of Na^+/H^+ exchange in the control of intracellular pH and cell membrane conductances in frog skin epithelium. *J. Gen. Physiol*. **92**, 793-810.

Hyrtl, J. (1838). Beobachtungen aus dem Gebiet der vergleichenden Gefäßlehre. II. Über den Bau der Kiemen der Fische. *Medizisches Jahrbuch* **15**, 232-248.

Kelly, S. P., Fletscher, M., Pärt, P. and Wood, C. M. (1999). Primary culture of rainbow trout branchial epithelium. *Comp. Biochem. Physiol*. **124A Supplement**, 36.

Kobayashi, H., Pelster, B. and Scheid, P. (1990). CO_2 back-diffusion in the rete aids O_2 secretion in the swimbladder of the eel. *Respir. Physiol*. **79**, 231-242.

Kramhoft, B., Lambert, I. H. and Hoffmann, E. K. (1988). Na^+/H^+ exchange in Ehrlich ascites tumor cells: activation by cytoplasmatic acidification and by treatment with cupric sulphate. *J. Memb. Biol*. **102**, 35-48.

Kuhn, W., Ramel, A., Kuhn, H. J. and Marti, E. (1963). The filling mechanism of the swimbladder. Generation of high gas pressures through hairpin countercurrent multiplication. *Experientia* **19**, 497-511.

Laurent, P. and Dunel-Erb, S. (1984). The pseudobranch: morphology and function. In *Fish Physiology*, vol. XB (ed. W. S. Hoar and D. J. Randall), pp. 285-323. Orlando, Florida: Academic Press.

Laurent, P., Goss, G. G. and Perry, S. F. (1994). Proton pumps in fish gill pavement cells? *Arch. Int. Physiol. Biochim. Biophys.* **102**, 77-79.

Lin, H., Pfeiffer, D. C., Vogl, A. W., Pan, J. and Randall, D. J. (1994). Immunolocalization of H^+-ATPase in the gill epithelia of rainbow trout. *J. Exp. Biol*. **195**, 169-183.

Lin, H. and Randall, D. (1995). Proton pumps in fish gills. In *Cellular and Molecular Approaches to Fish Ionic Regulation*, vol. 14 (ed. C. M. Wood and T. J. Shuttleworth), pp. 229-255. San Diego, New York: Academic Press.

Maetz, J. (1956). Le role biologique de l'anhydrase carbonique chez quelques téléostéens. *Suppléments au Bulletin biologique de France et de Belgique Les presses universitaires de France*, 1-129.

McConnell, H. M., Owicki, J. C., Parce, J. W., Miller, D. L., Baxter, G. T., Wada, H. G. and Pitchford, S. (1992). The cytosensor microphysiometer: Biological applications of silicon technology. *Science* **257**, 1906-1912.

Mobasheri, A., Avila, J., Cozar-Castellano, I., Brownleader, M. D., Treva, M., Francis, M. J., Lamb, J. F. and Martin-Vasallo, P. (2000). Na^+, K^+-ATPase isozyme diversity; comparative biochemistry and physiological implications of novel functional interactions. *Biosci. Rep.* **20,** 51-91.

Müller, J. (1839). Vergleichende Anatomie der Myxinoiden. III. Über das Gefässystem. *Abh. Dtsch. Akad. Wiss. Berlin* **1839**, 175-303.

Niederstätter, H. and Pelster, B. (2000). Expression of two vacuolar-type ATPase B subunit isoforms in swimbladder gas gland cells of the European eel: nucleotide sequences and deduced amino acid sequences. *Biochim. Biophys. Acta Gene Struct. Express.* **1491**, 133-142.

Owicki, J. C. and Parce, J. (1992). Biosensors based on the energy metabolism of living cells: the physical chemistry and cell biology of extracellular acidification. *Biosens. Bioelectron.* **7**, 255-272.

Owicki, J. C., Parce, J. W., Kercso, K. M., Sigal, G. B., Muir, V. C., Venter, J. C., Fraser, C. M. and McConnell, H. M. (1990). Continuous monitoring of receptor-mediated changes in the metabolic rates of living cells. *Proc. Natl. Acad. Sci. USA* **87**, 4007-4011.

Pärt, P. and Bergström, E. (1995). Primary cultures of teleost branchial epithelial cells. In *Cellular and Molecular Approaches to Fish Ionic Regulation*, vol. 14 (ed. C. M. Wood and T. J. Shuttleworth), pp. 207-227. San Diego, New York: Academic Press.

Pärt, P., Norrgren, L., Bergström, E. and Sjöberg, P. (1993). Primary cultures of epithelial cells from rainbow trout gills. *J. Exp. Biol*. **175**, 219-232.

Pelster, B. (1995). Mechanisms of acid release in isolated gas gland cells of the European eel *Anguilla anguilla*. *Am. J. Physiol*. **269**, R793-R799.

Pelster, B. (1997). Buoyancy at depth. In *Deep-Sea Fish* (ed. D. Randall and A. P. Farrell), pp. 195-237. San Diego: Academic Press.

Pelster, B. (2002). The generation of hyperbaric oxygen tensions in fish. *News Physiol. Sci*. **16**, 287-291.

Pelster, B. and Randall, D. J. (1998). The physiology of the Root effect. In *Fish Respiration* (ed. S. F. Perry and B. L. Tufts), pp. 113-139. San Diego: Academic Press.

Pelster, B. and Weber, R. E. (1990). Influence of organic phosphates on the Root effect of multiple fish haemoglobins. *J. Exp. Biol*. **149**, 425-437.

Perry, S. F. (1997). The chloride cell: structure and function in the gills of freshwater fishes. *Ann. Rev. Physiol*. **59**, 325-347.

Perry, S. F., Beyers, M. L. and Johnson, D. A. (2000). Cloning and molecular characterisation of the trout (*Oncorhynchus mykiss*) vacuolar H^+-ATPase B subunit. *J. Exp. Biol*. **203**, 459-470.

Ruggiero, F. P. and Sheffield, J. B. (1998). The use of avidin as a probe for the distribution of mitochondrial carboxylases in developing chick retina. *J. Histochem. Cytochem*. **46**, 177-183.

Sötz, E., Niederstätter, H. and Pelster, B. (2002). Determinants of intracellular pH in gas gland cells of the swimbladder of the European eel *Anguilla anguilla*. *J. Exp. Biol*. **205**, 1069-1075.

Steen, J. B. (1963). The physiology of the swimbladder in the eel *Anguilla vulgaris*. III. The mechanism of gas secretion. *Acta Physiol. Scand*. **59**, 221-241.

Sullivan, G. V., Fryer, J. M. and Perry, S. F. (1996). Localization of mRNA for the proton pump (H^+-ATPase) and Cl^-/HCO_3^- exchanger in the rainbow trout gill. *Can. J. Zool*. **74**, 2095-2103.

Wagner, S., Vogel, R., Lietzke, R., Koob, R. and Drenckhahn D. (1987). Immunochemical characterization of a band 3-like anion exchanger in collecting duct of human kidney. *Am. J. Physiol*. **253,** F213-F221.

Waser, W., Berenbrink, M. and Heisler, N. (1998). Oxygen supply to the fish retina. *Zoology* **101**, 69.

Wilson, J. M., Laurent, P., Tufts, B. L., Benos, D. J., Donowitz, M., Vogl, A. W. and Randall, D. J. (2000). NaCl uptake by the branchial epithelium in freshwater teleost fish: an immunological approach to ion-transport protein localization. *J. Exp. Biol*. **203**, 2279-2296.

Wilson, J. M., Randall, D. J., Donowitz, M., Vogl, A. W. and Ip, A. K.-Y. (2000). Immunolocalization of ion-transport proteins to branchial epithelium mitochondria-rich cells in the mudskipper (*Periophthalmodon schlosseri*). *J. Exp. Biol*. **203**, 2297-2310.

Wittenberg, J. B. and Haedrich, R. L. (1974). The choroid rete mirabile of the fish eye. II. Distribution and relation to the pseudobranch and to the swimbladder rete mirabile. *Biol. Bull*. **146**, 137-156.

Wittenberg, J. B. and Wittenberg, B. A. (1962). Active secretion of oxygen into the eye of fish. *Nature* **194**, 106-107.

Wittenberg, J. B. and Wittenberg, B. A. (1974). The choroid rete mirabile of the fish eye. I. Oxygen secretion and structure: Comparison with the swimbladder rete mirabile. *Biol. Bull*. **146**, 116-136.

Wood, C. M. and Pärt, P. (1997). Cultured branchial epithelia from freshwater fish gills. *J. Exp. Biol*. **200**, 1047-1059.

Wood, C. M. and Pärt, P. (2000). Intracellular pH regulation and buffer capacity in CO_2/HCO_3^- –buffered media in cultured epithelial cells from rainbow trout gills. *J. Comp. Physiol*. **170B**, 175-184.